

Accepted: ApJ, November 2011

Multiwavelength Characteristics of Period-Luminosity Relations

Barry F. Madore & Wendy L. Freedman

*Observatories of the Carnegie Institution of Washington
813 Santa Barbara St., Pasadena, CA 91101*

barry@obs.carnegiescience.edu, wendy@obs.carnegiescience.edu

ABSTRACT

We present a physically motivated explanation for the observed, monotonic increase in slope, and the simultaneous (and also monotonic) decrease in the width/scatter of the Leavitt Law (the Cepheid Period-Luminosity (PL) relation) as one systematically moves from the blue and visual into the near and mid-infrared. We calibrate the wavelength-dependent, surface-brightness sensitivities to temperature using the observed slopes of PL relations from the optical through the mid-infrared, and test the calibration by comparing the theoretical predictions with direct observations of the wavelength dependence of the scatter in the Large Magellanic Cloud Cepheid PL relation. In doing so we find the slope of the Period-Radius (PR) relation is $c = 0.724 \pm 0.006$. Investigating the effect of differential reddening suggests that this value may be overestimated by as much as 10%; however the same slope of the PR relation fits the (very much unreddened) Cepheids in IC 1613, albeit with lower precision. The discussion given is general, and also applies to RR Lyrae stars, which also show similarly increasing PL slopes and decreasing scatter with increasing wavelength.

Subject headings: Stars: variable: Cepheids – Stars: fundamental parameters – Stars: variable: RR Lyrae

1. Introduction

The Period-Luminosity (PL) relation for Classical Cepheids is a 2-dimensional projection of the higher-order Period-Luminosity-Color (PLC) relation. The PLC relation, in turn, is a finite portion of a plane, a so-called strip, embedded in the 3-dimensional space of period, luminosity and color. This strip is defined and delimited by physical limits (on temperature and luminosity) within which the atmospheres of these stars are found to be pulsationally unstable. A graphical representation of how these various projections arise and are inter-related was first given in Figure 3 of Madore & Freedman (1991). From this perspective it is clear that the width and orientation of the PLC strip in 3-dimensional space will have direct and profound influence on the measured properties of the 2D relations, projected and multiply transformed to observable (wavelength-dependent) quantities (magnitudes and colors).

It has long been known that the intrinsic width of the Cepheid Period-Luminosity (PL) relation (as commonly parameterized by its formal dispersion) *decreases* as a function of increasing wavelength (see, for example, Madore & Freedman 1991 for the optical, McGonegal et al. 1982 for the near-infrared; and more recently Madore et al. 2009 for applications in the mid-infrared). What is less commonly noted, although just as obvious, is the fact that the slope of the Cepheid PL relation does the opposite, and *increases* systematically with increased wavelength. This anti-correlation of slope and dispersion is shown in Figure 1, which is an updated and expanded version of a plot first presented as Figure 6 in Madore & Freedman (1991). Scatter is the quantity of most interest when any such relation is being used for distance determinations. The slope, on the other hand, is of little or no consequence in most practical applications. In the following, however, we show that the behavior of these two quantities, slope and scatter, share a common physical explanation, and that they can be readily understood (i.e., predicted) from first principles. Moreover, there may indeed be some practical implications arising from this realization.

2. An Analytic Approach

The total luminosity of a radiating object is the product of its total (radiating) area times the mean surface brightness of that area. Generalizing the Stefan-Boltzmann Law to a monochromatic (rather than bolometric) observation can be done by parameterizing the surface brightness by some power, a_λ , of the effective temperature, T_e . Thus, the entire (i.e., infinite) planar extent of the color-magnitude diagram is mapped by

$$M_\lambda = -2.5 \log R^2 - 2.5 \times a_\lambda \log T_e + b_\lambda \dots \quad (1)$$

where R is the radius of the star and λ is the wavelength of the observational bandpass. By imposing the following linear “constraints” on the above equation one can then define the (red/cool and blue/hot) boundaries of the instability strip: $\log R = c \log P + d$ and $\log T_e = -e \log P + f$, where P is the period, and where it is to be noted that a_λ, c and e are all numerically positive quantities. Applying these external constraints to the master equation (1) above (where f_{red} and f_{blue} are respectively the red and blue intercepts of the blue and red boundaries of the instability strip) gives

$$M_\lambda^{red} = [-5 c + 2.5 e a_\lambda] \log P - 2.5 \times [a_\lambda \times f_{red}] + b_\lambda - 5 d \dots \quad (2a)$$

$$M_\lambda^{blue} = [-5 c + 2.5 e a_\lambda] \log P - 2.5 \times [a_\lambda \times f_{blue}] + b_\lambda - 5 d \dots \quad (2b)$$

The full (wavelength-dependent) magnitude widths of the respective PL relations, $|M_\lambda|$ (which are directly related and proportional to their intrinsic dispersions) are then found to be

$$|M_\lambda| = 2.5 \times a_\lambda |f_{blue} - f_{red}| \dots \quad (3)$$

Moreover, the (central) ridge-line equation of the mean PL relation becomes $(M_\lambda^{red} + M_\lambda^{blue})/2$ or

$$M_\lambda^{mean} = [-5 c + 2.5 e a_\lambda] \log P - 2.5 [a_\lambda \times f_{mean}] + b_\lambda - 5 d] \dots \quad (4)$$

where $F_{mean} = (f_{red} + f_{blue})/2$.

The slopes of the corresponding (wavelength-dependent) PL relations are then

$$\Delta M_\lambda / \Delta \log P = A_\lambda = -5 c + 2.5 e a_\lambda \dots \quad (5)$$

The explicit dependence¹ of both the slope (through Equation 5) and the width/scatter (through Equation 3) on the same wavelength-dependent term, a_λ , now becomes clear.

¹For mathematical simplicity the above derivation implicitly assumes that the red and blue boundaries of the instability strip are parallel. The referee has pointed out that this may in fact not be the case, citing both theoretical (Bono et al. 2000) and observational evidence (Tammann et al. 2003) to the contrary. However the main point of this exercise is to show that a_λ is common to both Equations 3 and 5. Whether

At fixed period, the total width of the PL relation at any given wavelength is simply the difference of Equations 2a and 2b, with the formal dispersion being a fixed multiplicative fraction of that width. A quick check shows that for a temperature width of the Cepheid instability strip of 700K (or $\Delta \log T_e = 0.05$) this corresponds to a color width of $\Delta(B-V) = 0.5$ mag and a corresponding magnitude width of $\Delta M_V = 0.8$ mag. If the stars are uniformly distributed within and across the strip this would correspond to a formal dispersion of $\sigma_V = 0.8/\sqrt{12} = \pm 0.23$ mag, which compares well with the observed dispersion of ± 0.27 mag for the LMC V-band PL relation as given in Madore & Freedman (1991).

the multiplicative factor “e” in Equation 5 is the average of two different numbers (non-parallel boundaries) or identical numbers (parallel boundaries) does not change the main conclusion.

2.1. A Graphical Approach

Figure 2 graphically captures the substance of the above cascade of equations, and visually illustrates just how the slopes of the PL relations and their widths/dispersions are coupled. Three PL relations are shown. The lower relation (labeled 3.6 at its terminal point to the right of the diagram) represents a long-wavelength PL relation having the characteristic low scatter and a steep slope. The thick parallel lines (flanking each of the mean PL relations) represent the upper and lower boundaries of the instability strip as projected into the period-luminosity plane. The light, dotted lines trace the mean relations. The thick dashed lines running diagonally across each of the PL relations represent lines of constant color/temperature.

It is important to note that the mapping of the PL relation at one wavelength into a PL relation as observed at another wavelength is solely dependent on the differential response of surface brightness to temperature across the respective wavelengths (as parameterized by a_λ in Equation 1). Hereafter color is taken to be synonymous with temperature. Given that the influence of temperature on surface brightness is known to be an increasingly sensitive function of decreasing wavelength, and given that temperature is itself a generally decreasing function of increasing period (longer-period Cepheids are generally cooler than their short-period counterparts), the mapping of the $3.6\mu\text{m}$ PL relation into the B band is shown by the two thick arrows of decreasing amplitude in going from hot temperatures (the arrow above the circled A) to cooler temperatures (the shorter arrow above the circled letter B). This systematic decrease in the vector’s magnitude with period (i.e., with mean temperature) is readily seen to be responsible for the systematic decrease in the slope of the PL relation in going from longer to shorter wavelengths (as explicitly given in Equation 5).

The vectors originating from points in the long-wavelength PL relation having the same temperature (as tracked by the dashed lines) have (by definition) exactly the same magnitude/length. Those vectors are shown terminating in the B-band PL relation just below the circled letters C and D. In other words, the slope of the lines of constant temperature, $\Delta\text{mag}/\Delta \log P$, are independent of the wavelength of the PL relation.

There is a fixed temperature difference in crossing the instability strip at a given period. This manifests itself as an increasingly larger magnitude width of the PL relation when observed at progressively shorter and shorter wavelengths (as can be seen in Equation 3).

There is also, as noted above, a general decrease in temperature (increase in color) along the PL relation as one increases the period. This results in the decreased magnitude of the correction for temperature as a function of period, which in turn manifests itself as a reduction of the overall slope of the PL relation as one goes to shorter and shorter

wavelengths.

The significant point here is that both of the above effects are controlled by a single physical parameter, the temperature. Accordingly, an increased slope of the Cepheid PL relation must be accompanied by a causally connected decrease in the intrinsic dispersion of the PL relation. The longer-wavelength PL relations will be steeper and their intrinsic scatter must be smaller than their shorter-wavelength counterparts.

3. A Calibration and Tests

Looking at Equation 4 more closely it is clear that the slope of the PL relation is made up of two linearly additive, but physically independent parts: (1) a constant term “ $5c$ ”, which is essentially the slope of the Period-Radius (PR) relation converted into a Period-Area (PA) relation, and then cast into a magnitude (i.e., by multiplying $\log R$ by 2×-2.5), and (2) the slope of the Period-Color relation (i.e., $-2.5 \times e \times (a_{\lambda_1} - a_{\lambda_2})$). It is this last term that contains the wavelength-dependent index, a_λ , characterizing the sensitivity of surface brightness to temperature variations for any given bandpass. If the (wavelength-independent) slope of the Period-Area relation is simply subtracted from the (wavelength-dependent) PL slopes one would be left with the purely wavelength-dependent, Period-Surface-Brightness relation (PSB) slope (for instance, transforming Equation 1 gives $M_\lambda + 2.5 \log R^2 = -2.5 \times a_\lambda \log T_e + b_\lambda$). Given that the constant of proportionality between slopes of the PSB relations and their respective dispersions must be the same number, independent of bandpass, we have then a means of determining the slope of the PA relation by demanding that the ratio of the PSB slope to PL dispersion must be constant and independent of wavelength.

Published values of the slope of the PR relation have been recently tabulated by Molinaro et al. (2010). Their own work suggests values of c ranging from 0.71 to 0.75, with historical values, drawn both from theory and observations, ranging more widely from 0.67 to 0.77. We now explore the run of the aforementioned proportionality constant with bandpass, parameterized by the input slope of the PR relation. The abscissa in Figure 3 which is the ratio of slope of the PL relation (Equation 5) to the dispersion in the PL relation (effectively Equation 3), will become independent of wavelength when the correct value of the scaled slope of the period-radius relation (i.e., $-5c$) is subtracted from the numerator, as given in Column 3 of Table 1. The intent is to find a slope of the PR relation that minimizes any residual trend of the proportionality constant with bandpass/wavelength. The circled dots in Figure 3 show that solution: no trend with bandpass (a formal slope of 0.000 ± 0.015) for an input value of $c = 0.721$, and a resulting scatter (± 0.009) that is exceedingly small.

In changing the slope of the PR relation to correspond to the Molinaro et al. limits, as given above, the two flanking solutions are realized. In both cases the dispersion is much enhanced, and there is a strong (and unphysical) trend seen with wavelength. This already small range in the PR slope (of only $\pm 3\%$ peak-to-peak) is now much more narrowly defined by the present study. Our final solution for the slope of the Cepheid Period-Radius relation and its error is $c = 0.724 \pm 0.006$.

The results of the above fitting, now adopting a PR slope of 0.724, are given in Table 1. The first column gives the bandpass, ranging from the blue to the mid-infrared, at which each fit was made. In the second column we list, in order of increasing wavelength, the published slopes, A_λ (equal to $-5c + 2.5ea_\lambda$; see equations (4) and (5)) of PL relations taken from a merger of Madore & Freedman (1991) for the optical, Persson et al. (2009) for the near-infrared, and Madore et al. (2009) for the mid-infrared. Column 3 gives the slope of the PSB relation obtained by subtracting the constant and wavelength-independent slope of the Period-Area relation (i.e., $-5 \times 0.724 = -3.62$) from the respective PL slopes (as given in Column 2) leaving $A_\lambda + 3.62 = 2.5ea_\lambda$. As already derived above, the multi-wavelength slopes of the PSB relations and the dispersion/widths of the PL relations must each be proportional to the same factor, a_λ . As can be seen in Figure 3 the incorrect choice of the slope of the PR relation very quickly leads to a divergence with wavelength in the prediction of the scale factor (that must be independent of wavelength) required to convert the slope to a scatter. This diagnostic diagram can therefore be used to find the wavelength-independent slope of the PR relation that best predicts the wavelength-dependent scatter in the observed PL relations from the optical BVRI to the near-infrared JHK bands.

As can be seen in Figure 3 for a value of $c = 0.72$ the Dispersion-to-Slope Ratio is independent of wavelength and has a value of 0.316. Using this proportionality factor we convert each of the wavelength-dependent PSB slopes to their corresponding wavelength-dependent PL-relation dispersions. These predicted dispersions are given in Column 4 of Table 1 (e.g., for a B-band Surface-Brightness slope of 1.19 the predicted dispersion in the B-band PL relation is $1.19 \times 0.316 = 0.376$ mag). Column 5 of Table 1 contains the observed PL relation dispersions, self-consistently taken from the same references cited above for the slopes of the PL relations. The correspondence of the predicted and observed dispersions is impressive. A slight divergence occurs in the mid-infrared where the observed dispersions are upper limits, due to the fact that these magnitudes were derived from only two random-phase observations and that they contain additional scatter imposed by the back-to-front depth and tilt of the LMC, whose Cepheids were used for these demonstrations.

An independent test using Cepheids in the Small Magellanic Cloud is compromised by the extremely large geometric, extrinsically correlated scatter due to the extension of the

SMC along our line of sight; however, the somewhat more distant galaxy IC 1613 can be used for this purpose. In the paper by Antonello et al. (2006) there are 48 Cepheids with complete BVRI photometry having periods ranging from 3 to 42 days. We have used these observations to derive the slopes and dispersions (the latter not having been published by these authors) for the four PL relations. The results are shown graphically in the lower left portion of Figure 2. The IC 1613 data are shown as filled dots enclosed by squares, each of which has an error bar derived from our calculated uncertainty on the slope at each wavelength. The points are plotted for an input value of the PR relation taken from the LMC solution. To within the uncertainties there is no obvious trend of the dispersion-to-slope ratio for the IC 1613 Cepheids using the LMC PR relation. There is, however, a systematic offset in the ratio which can be directly attributed to a narrower sampling of the Cepheid instability strip by the IC 1613 Cepheids. The conclusion remains that the slope of the PR relation is identical for these two galaxies. Extending the test to other systems with a wider range of metallicities will be of interest. However, until GAIA produces parallaxes for a sufficiently large sample of Milky Way Cepheids calibrating this relation in the galaxy will have to be postponed until secure reddenings and accurate distances are available for more than a handful of galactic Cepheids.

3.1. The Effects of Differential Reddening

Differential reddening with the sample of (LMC) Cepheids used in this study will contribute to the observed scatter in the respective PL relations. This extrinsic contribution will also decrease in its magnitude as a function of increasing wavelength, in parallel with the decreased intrinsic width with wavelength driven temperature sensitivity. Here we explore the systematics of differential reddening on this study.

Independent estimates of the total line-of-sight dispersion in the reddening to the LMC (e.g., Grieve & Madore 1986) suggests that σ_{A_V} is on the order of ± 0.10 mag. We have progressively removed (in quadrature) increasing amounts of possible differential reddening bracketting this value, and iteratively re-solved for the input slope of the PR relation using the minimum variance condition on the derived value the scaling factor “c”. This was followed by visually confirming with the wavelength plots (individually corresponding to Figure 3) that there was no residual correlation with wavelength. For a one-sigma dispersion in the putative differential reddening of $\sigma_{A_V} = 0.10$ mag the minimum dispersion on “c” was found to be ± 0.0040 for $c = 0.754$. Recall that the minimum dispersion for the solution with no differential reddening correction was marginally smaller (at a value of 0.0036 for $c = 0.724$). The σ_{A_V} correction of 0.10 mag results in a 4% change in the derived value of the

slope of the PR relation. Increasing the differential reddening correction to $\sigma_{A_V} = 0.20$ mag more than doubles the error on the fit taking it to 0.0074 for a minimization value of $c = 0.792$, which is now a 10% systematic shift in the derived value of the slope of the PR relation.

We conclude that correcting for a reasonable amount of differential reddening (i.e., $\sigma_{A_V} = 0.10$ mag.) acts to systematically increase the slope of the derived PR relation (but by only 4% in this instance) at the expense of decreased precision in the final fit. However, there is an alternative approach to dealing with differential reddening.

The Wesenheit function, $W = V - R \times (B - V)$ (Madore 1976) is designed to eliminate the effects of dust (total and differential) by a judicious choice of scaled colors and magnitudes, adjusted to have reddening (in the color) exactly cancel extinction (in the magnitude), where $R = A_V/E(B - V)$. But, that same formalism of combining colors and magnitudes can alternatively be used to target and scale out the temperature variation across the PL relation (at fixed period), such that $W' = V - \beta \times (B - V)$ where β is the slope of lines of constant period crossing the Cepheid instability strip within the color-magnitude diagram. In the absence of differential reddening W' would have minimum dispersion when its slope is equal to the slope of the PA relation, namely “5c”.

For the LMC Cepheids with B and V photometry we have examined the run of dispersion in W' as a function of β . It reaches a minimum dispersion of $\sigma_{W'} = \pm 0.13$ mag for $\beta = 2.15$, where the slope of the W' -Period relation is determined to be -3.48 ± 0.04 . This would then correspond to a PR relation slope of $c = 0.70 \pm 0.01$. Noting that the minimized scatter in W' is still larger than the scatter expected for the PA relation alone, and larger than the scatter seen at longer wavelengths (± 0.08 mag), it is probable that photometric errors, combined with residual reddening effects, are limiting this determination. Nevertheless, the value of the slope of the PR relation inferred from this one application is also gratifyingly close to recent direct determinations.

4. Discussion and Conclusions

While it could have been predicted, it is only now that we know that the decreased width and the increased slope of the Cepheid PL relation, as a function of increased observing wavelength, is inevitable. Both effects are driven by the wavelength-dependent temperature sensitivity of stellar surface brightness. At the longest wavelengths the PL relation asymptotically parallels the (wavelength-independent) PR relation; at shorter wavelengths the PL relation is increasingly dominated by the (highly wavelength dependent) surface-brightness

sensitivity to temperature.

It is of interest to use aspects of this formalism to put constraints on the slope of the PR relation. Since the dispersion must be non-negative the slope of the PA relation cannot be shallower than the steepest (longest-wavelength) slope of the PL relation. The steepest slope in Table 1 is -3.49 seen at $8.0\mu\text{m}$. This would require that the slope of the PR relation be steeper than $c = -0.70$, since there must still be at least one power of T_e flattening the slope of the PL relation, even at the longest-wavelength limit. Examination of the minimum dispersion solution of the generalized Wesenheit function gives a value of $c = -0.70$. And, more comprehensively, by requiring that the run of dispersion-to-slope be independent of wavelength gives for LMC Cepheids $c = -0.724 \pm 0.006$, a value that also fits the Cepheids in IC 1613.

The implications of this discussion are not confined to Classical Cepheids. For example, the somewhat surprising (at the time) discovery by Longmore, Fernley & Jameson (1986) that RR Lyrae stars obey a fairly steep and tightly-defined PL relation in the near infrared, as compared to the same stars whose optical magnitudes show almost no dependence on period, is directly explained by the same argument given here in the main text. Inspection of the plots given by Longmore, Fernley & Jameson (1986) would suggest that the scatter in the derived absolute magnitudes for RR Lyrae stars decreases by at least a factor of two in going from V to K as the slope of the PL relation rises from being essentially flat at V to having a value of about -2.5 at K. This observed trend is re-enforced and confirmed by multi-wavelength modelling of RR Lyrae stars by Catelan, Pritzl & Smith (2004) whose Figure 2 dramatically tracks the systematic change of increasing slope and decreasing scatter occurring progressively from the ultraviolet to the near infrared.

One note of caution is necessary. As the referee of this paper has suggested additional (magnitude) scatter may compromise these correlations in the case of RR Lyrae stars “caused by off-ZAHB evolution (which depends in turn on HB type) rather than intrinsic effects.” The same caveat may apply to the Cepheids themselves given that stars of a given mass may make several crossings of the instability strip giving rise to first-, second- and third-crossing scatter in period at a given luminosity and temperature.

Finally, we note that changes in the mapping of temperature to surface brightness might be modulated by additional physics, such as line blanketing changes in response to atmospheric metallicity variations, or surface gravity, effects especially in the near ultraviolet, etc. As such, both the intrinsic width and the slope of the Cepheid PL relation will each be physically (and mathematically) forced to respond in a well determined fashion. If the slope is thought to be increased, say, at a given wavelength because of a metallicity difference, then the prediction is that the intrinsic dispersion will be decreased, and vice versa. However,

uncertainties in differential reddening within any given Cepheid sample will always make these higher-order tests challenging.

Acknowledgements

We thank Eric Persson, Vicky Scowcroft and Mark Seibert for providing much valued comments on early drafts of this paper.

References

- Antonello, E., Fossati, L., Fugazza, D, Mantegazza, L., & Gieren, W. 2006, *Å*, 445, 901
- Bono, G., Castellani, V., & Marconi, M. 2000, *ApJ*, 529, 293
- Catelan, M., Pritzl, B.J., & Smith, H.A. 2004, *ApJS*, 154, 633
- Grieve, G.R., & Madore, B.F. 1986, *ApJS*, 62, 427
- Longmore, A.J., Fernley, J.A. & Jameson, R.F. 1986, *MNRAS*, 220, 279
- Madore, B.F. 1976, *Royal Greenwich Observatory Bulletins*, 182, 153
- Madore, B.F. 2009, *ApJ*, 298, 304
- Madore, B.F., & Freedman, W.L. 1991, *PASP*, 103, 933
- Madore, B.F., Freedman, W.L., Rigby, J., Persson, S.E., Sturch, L., & Mager, V. 2009, *ApJ*, 695, 988
- McGonegal, R., McAlary, C.W., Madore, B.F. & McLaren, R.A. 1982, *ApJ*, 257, L33
- Molinaro, R., Ripepi, V., Marconi, M., Bono, G., Lub, J., Pedicelli, S., & Pel, J. W. 2010, *astro-ph:1012.4376*
- Persson, S.E., et al. 2009, *AJ*, 128, 2239
- Tammann, G.A., Sandage, A.R., & Reindl, B. 2003, *Å*, 404, 423

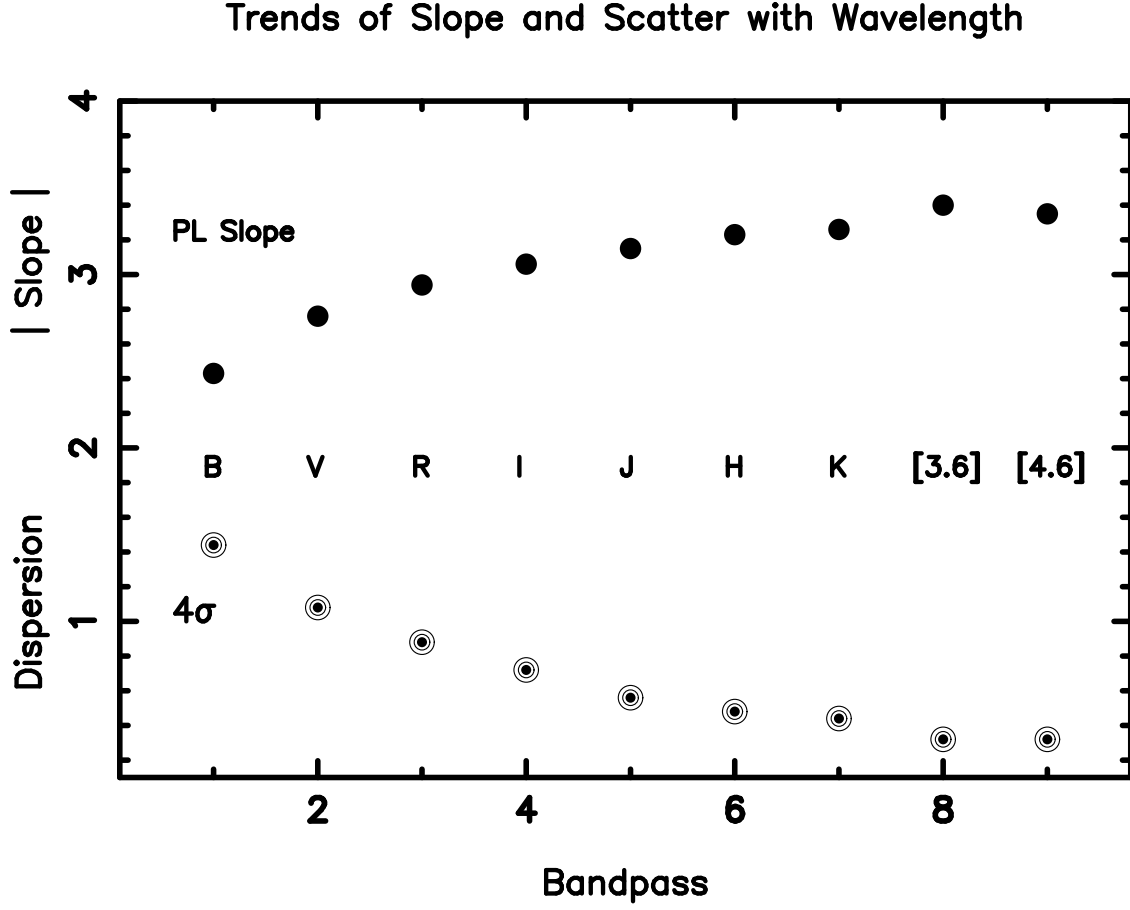


Fig. 1.— Correlated trends in the observed slopes and widths of multi-wavelength Period-Luminosity relations as a function of wavelength. The upper portion of the panel shows the monotonic *increase* in the slope of the Cepheid PL relation with increasing wavelength of the bandpass. The lower portion of the figure shows the systematic *decrease* of the dispersion in the PL relation as a function of increasing wavelength.

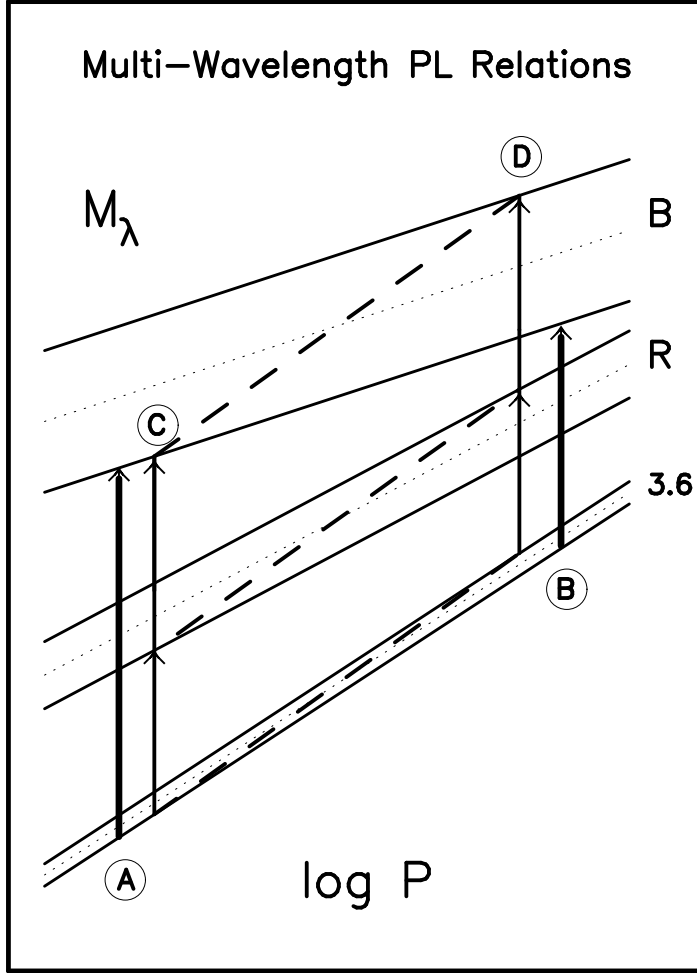


Fig. 2.— Multi-Wavelength Period-Luminosity Relations. The three sets of upward-sloping solid parallel lines represent the boundaries of the Cepheid instability strip as projected into the period-luminosity plane at three different wavelengths (B, R and $3.6 \mu\text{m}$). A line of constant period is vertical; a line of constant luminosity is horizontal. Not so obvious is the fact that a line of constant color/temperature is an upward sloping diagonal line, shown by dashed broken lines in each of the three PL relations illustrated here.. The heavy vertical line above the circled letter ‘A’, to the left (i.e. toward shorter periods) in the diagram, represents the large effect (at higher temperatures) of transforming the temperature sensitivity of the surface brightness from the mid-infrared ($3.6 \mu\text{m}$) to the B band. The shorter, heavy vertical line above the circled letter ‘B’, shows the decreased effect of transforming the surface brightness at lower temperatures from the mid-IR to the B band. This differential effect causes the B-band PL relation to have a systematically shallower slope than that of the mid-IR PL relation. The heightened sensitivity of the B band to fixed temperature differences across the instability strip at any given period results in the significantly increased width of the B-band PL relation in comparison to the much smaller temperature-induced magnitude width at mid-IR wavelengths. The width increase and the slope decrease are both controlled by the same physics (the temperature sensitivity of the monochromatic surface brightness); they are deterministically coupled in the sign and magnitude of their variations.

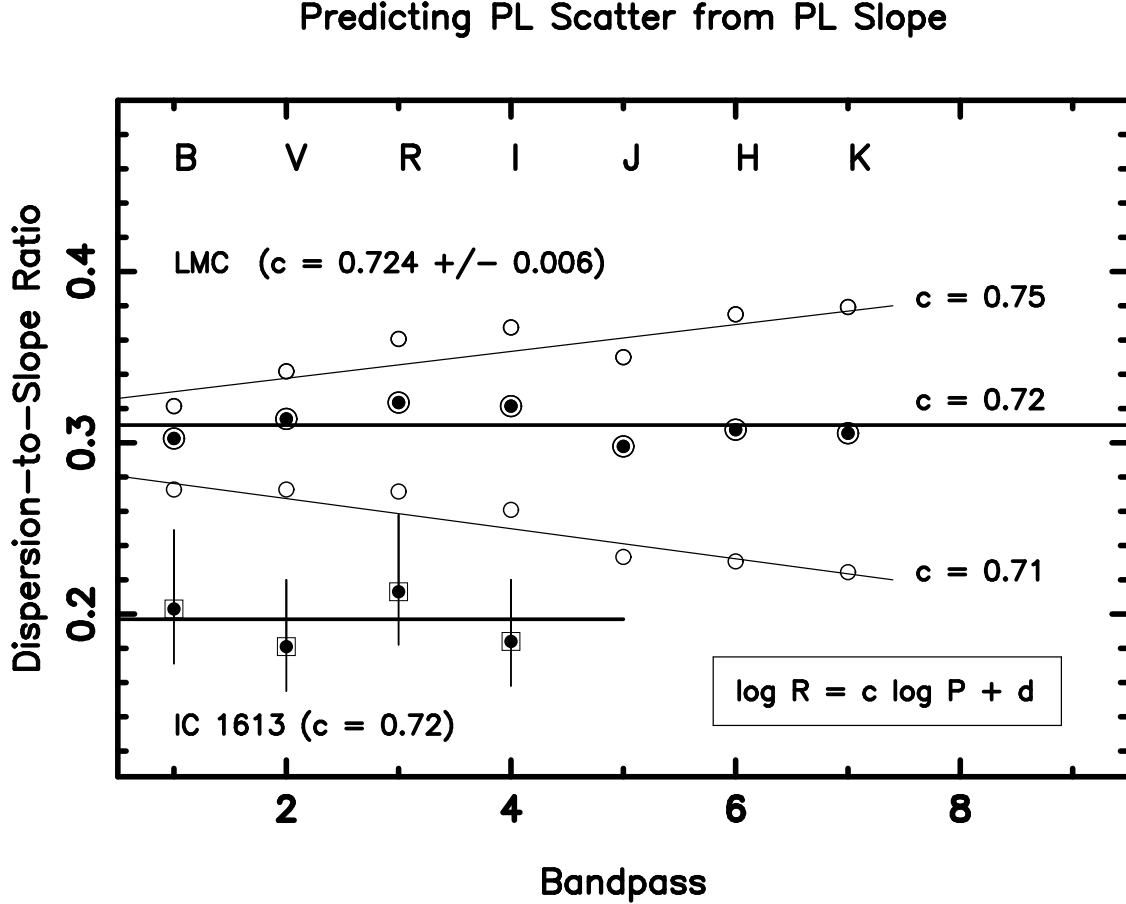


Fig. 3.— The ratio of the dispersion in the Period-Luminosity relation to the corresponding slope of the Period Surface-Brightness relation, parameterized by the slope of the Period-Radius relation, “ c ”, and plotted as a function of bandpass (running from B through K as indicated across the top of the plot). For the LMC data (top) a value of $c = 0.724 \pm 0.006$ gives the wavelength-independent (flat) correlation shown by the circled dots. The two flanking solutions (open circles) illustrate solutions resulting from adopting the recently published extreme values of the slope of the PR relation ($c = 0.71$ and 0.75) as given by Molinaro et al. (2010). In the bottom left corner of the plot are shown BVRI data (dot-filled squares) for Cepheids in IC 1613. They too have a flat correlation with wavelength for the same input value of the LMC PR relation slope; however, the offset indicates that the width of the IC 1613 instability strip appears to be about 30% narrower than the LMC.

Table 1. Predicted and Observed Wavelength-Dependent PL Dispersions

| Band | PL Slope $A_\lambda(\text{obs})$ | SB Slope $A_\lambda(\text{obs}) + 3.62$ | $\sigma_{\text{predicted}}$ (mag) | $\sigma_{\text{obs.}}$ (mag) |
|-------|-------------------------------------|--|--------------------------------------|---------------------------------|
| (1) | (2) | (3) | (4) | (5) |
| B | -2.43 | 1.19 | 0.376 | 0.36 |
| V | -2.76 | 0.86 | 0.272 | 0.27 |
| R | -2.94 | 0.68 | 0.215 | 0.22 |
| I | -3.06 | 0.56 | 0.177 | 0.18 |
| J | -3.15 | 0.47 | 0.149 | 0.14 |
| H | -3.23 | 0.39 | 0.123 | 0.12 |
| K | -3.26 | 0.35 | 0.111 | 0.11 |
| [3.6] | -3.40 | 0.22 | 0.070 | <0.08 |
| [4.5] | -3.35 | 0.27 | 0.085 | <0.08 |
| [5.8] | -3.44 | 0.18 | 0.057 | <0.08 |
| [8.0] | -3.49 | 0.13 | 0.041 | <0.08 |